SIMULATION OF PERFORMANCE ON MULTI-QUANTUM-WELL VIOLET InGaN LASER DIODE AND ANALYSIS OF ITS OUTPUT FOR DIGITAL MODULATION

RAFID A. ABDULLAH

UNIVERSITI SAINS MALAYSIA
2010

SIMULATION OF PERFORMANCE ON MULTI-QUANTUM-WELL VIOLET InGaN LASER DIODE AND ANALYSIS OF ITS OUTPUT FOR DIGITAL MODULATION

by

RAFID A. ABDULLAH

Thesis submitted in fulfillment of the requirements
for the degree of
Doctor of Philosophy

September 2010

ACKNOWLEDGMENTS

First of all, I would like to thank Allah for granting me health, patience and willing to finish this research. I would also like to express my deepest appreciation to my adviser, Professor Dr. Kamarulazizi Ibrahim for his feedback, guidance and comments on my work.

A special thank goes to Dr. Muzahim I. Azawe for his continuous encouragement. I also appreciate my Ph.D. colleagues for the group discussion. My thanks go to the staff members of the Nano-optoelectronic Research and Technology laboratory (N.O.R) at School of Physics in Universiti Sains Malaysia.

TABLE OF CONTENTS

CHAPTER 1: INTRODUCTION

CHAPTER 2: THEORETICAL FRAMEWORK

CHAPTER 3: SIMULATION METHODOLOGY

CHAPTER 4: PERFORMANCE OF MQW VIOLET InGaN LASER DIODE

CHAPTER 5: OUTPUT ANALYSIS AND DIGITAL MODULATION

CHPTER 6: CONCLUSIONS AND FUTURE WORK

APPENDIXES

LIST OF TABLES

LIST OF FIGURES

LIST OF ABBREVIATIONS

BD	Blu-ray Disc
BER	Bit Error Rate
BL	Blocking Layer
CW	Continuous Wave
DC	Direct Current
DH	Double-Heterostructure
DQE	Differential Quantum Efficiency
DQW	Double Quantum Well
DVD	Digital Versatile Disc
ELO	Epitaxial Lateral Overgrowth
Eq.	Equation
ISE TCAD	Integrated System Engineering Technology Computer Aided Design
LD	Laser Diode
LD1	Multi-quantum-well violet InGaN LD with a ternary AlGaN BL
LD2	Multi-quantum-well violet InGaN LD with a quaternary AlInGaN BL
LED	Light Emitting Diode
L-I	Light output power-Current
L-I-V	Light output power-Current-Voltage
LEEBI	Low-Energy Electron-Beam Irradiation
MBE	Molecular Beam Epitaxy
MATLAB	MATrix LABoratory
MOCVD	Metal Organic Chemical Vapor Deposition
MQW	Multi-Quantum-Well
OCF	Optical Confinement Factor

PL	Photoluminescence
QCSE	Quantum Confined Stark Effect
QW	Quantum Well
QW-DFB	Quantum Well-Distributed FeedBack
RO	Relaxation Oscillation
RT	Room Temperature
SCH	Separate Confinement Heterostructure
SL	Superlattice
VCSEL	Vertical Cavity Surface Emitting Laser
UV	Ultraviolet
OOK	On/Off Keying

LIST OF SYMBOLS

a	Lattice constant
B	Bit rate
b	Band gap bowing parameter
c	Speed of the light in space
d	Thickness of the quantum well
E	Electric field
E_g	Band gap energy
e_{ij}	Piezoelectric constant
f_r	Frequency of the relaxation oscillation
g_{th}	Threshold gain
g_o	Slope gain constant
h	Planck constant
I	Current of the laser diode
I_b	Bias current
$I_{ip.}$	Input current
I_p	Current pulse
I_m	Modulation current
I_{th}	Threshold current of the laser diode
J_o	Carrier density at transparency
J_{th}	Threshold current density of the laser diode
k	Boltzmann constant
L	Laser diode cavity length
m	Mass of particle
m_o	Electron effective mass

m_{hh}	Heavy hole effective mass
m_{lh}	Light hole effective mass
m^*	Effective mass of the particle
$N(t)$	Carrier density
N_{th}	Carrier density at threshold
N_o	Carrier density at transparency
$\bar{N}$	Carrier density at steady-state
n	Refractive index
n_{sp}	Population inversion factor
P	Output power of the laser diode
P_{av}	Average of optical power
P_i	Electric polarization
P_{sp}	Spontaneous polarization
P_o	Optical power corresponding to a logic zero
P_1	Optical power corresponding to a logic one
Q	Physical parameter
q	Electron element charge
R	Reflectivity of the laser diode mirror
r_e	Extinction ratio
$S(t)$	Photon density
S_{on}	First reaches steady-state photon density
$\bar{S}$	Photon density at steady-state
T	Absolute temperature
T_B	Bit period
T_o	T-zero

t_d	Turn-on delay time
t_{off}	Turn-off time
t_{on}	Turn-on time
v_a	Active region volume
w	Thickness of the active region
α	Linewidth enhancement factor
α_i	Internal loss
α_m	Mirror loss
β	Spontaneous emission factor
$\delta_e(r_e)$	Power penalty
$\Phi(t)$	Optical phase
Γ	Optical confinement factor
ε	Non-linear gain coefficient
ε_{ij}	Strain
η_d	Differential quantum efficiency
η_i	Internal quantum efficiency
λ	Wavelength of LD
$\lambda_{de.}$	De Broglie wavelength
τ_n	Carrier lifetime
τ_{nr}	Non-radiative carrier lifetime
τ_p	Photon lifetime
τ_r	Radiative carrier lifetime
υ	Laser diode frequency

SIMULASI PRESTASI DIOD LASER UNGU TELAGA KUANTUM BERGANDA InGaN DAN ANALISA OUTPUT UNTUK MODULASI DIGIT

ABSTRAK

Kajian simulasi dan teoritikal ini telah dibahagikan kepada dua bahagian utama. Bahagian pertama mengfokuskan kepada prestasi diod laser ungu telaga kuantum berganda InGaN; manakala, bahagian kedua pula mengfokuskan kepada analisis output laser ini untuk digunakan sebagai modulasi digit.

Dua program telah digunakan iaitu program perisian simulasi ISE TCAD (Integrated System Engineering Technology Aided Design) dan juga program MATLAB. Penyelidik telah mengabungkan pengunaan dua program ini iaitu simulasi ISE TCAD dan program MATLAB untuk menghasilkan satu kaedah baru dalam proses simulasi modulasi digit untuk LD.

Objektif utama kajian yang dijalankan ini adalah untuk menghasilkan arus ambang yang rendah dan lengkung bebas pintal kuasa-arus (L-I) untuk bagi diod laser ungu telaga kuantum berganda InGaN dengan panjang gelombang terpancar menghampiri 405 nm, dan analisi output laser ini bertujuan untuk modulasi digi.

Prestasi diod laser ungu telaga kuantum berganda InGaN telah dicapai setelah mengoptimumkan kawasan aktif, lapisan sekatan dan juga panjang lubang. Diod laser ungu telaga kuantum berganda InGaN dengan telaga dwi-kuantum telah digunakan sebagai struktur asas. Kesan daripada ketebalan telaga kuantum, ketebalan sawar dan jenis ke atas ciri elektrikal, optikal dan kekutuban terbina dalam (build-in polarization) telah dikaji. Lengkung bebas pintal L-I dengan nilai arus ambang yang rendah (16.42 mA) dan kuasa output yang tinggi (64.2 mW) telah diperolehi dengan nilai telaga kuantum dan ketebalan pemampan pada 2.5 dan 5 nm masing-masing.

Kekutuban terbina dalam telah dibuktikan mempunyai kebergantungan terhadap ketebalan telaga kuantum serta ketebalan dan jenis sawar.

Kesan daripada lapisan sekatan AlInGaN kuartener ke atas sifat LD telah dikaji secara ekstensif. Arus ambang untuk LD telah dikurangkan daripada 16.42 mA kepada 13.76 mA apabila mengambilkira kuartener sebagai lapisan sekatan berbanding AlGaN pertigaan sebagai lapisan sekatan. Peningkatan taburan kepadatan pembawa di antara dua telaga kuantum telah diperolehi dengan lapisan sekatan AlInGaN kuartener.

Analisis terhadap output diod laser ungu telaga kuantum berganda InGaN yang dihasilkan telah diperolehi dan parameter diod laser yang diperlukan untuk kajian dan analisis terhadap respon denyut untuk modulasi digit telah dihitung melalui analisis output, penyelesaian persamaan kadar diod laser, dan beberapa kerja eksperimen. Parameter untuk modulasi digit yang telah dikaji dan diperolehi adalah ayunan santaian, kekerapan ayunan santaian, masa buka dan tutup, dan nisbah pemusnahan. Diod laser ungu telaga kuantum berganda InGaN dengan lapisan sekatan AlInGaN kuartener telah memperlihatkan sifat modulasi digital yang lebih baik berbanding diod laser dengan lapisan sekatan AlGaN pertigaan.

Keseluruhannya, di dalam hasilan kajian simulasi ini, didapati ia sejajar dan bertepatan dengan beberapa kerja eksperimen di dalam kajian persuratan.

SIMULATION OF PERFORMANCE ON MULTI-QUANTUM-WELL VIOLET InGaN LASER DIODE AND ANALYSIS OF ITS OUTPUT FOR DIGITAL MODULATION

ABSTRACT

This simulation and theoretical study is divided into two parts. Part one focuses on the performance of multi-quantum-well (MQW) violet InGaN laser diode (LD); whereas, part two focuses on the analysis of the output of this laser for the purpose of digital modulation.

Two programs have been utilized. They are ISE TCAD (Integrated System Engineering Technology Computer Aided Design) simulator and MATLAB program. The researcher has coupled ISE TCAD simulator with MATLAB program as a new method for the purpose of simulation of digital modulation of the LD.

The main objectives of this study are to obtain a low threshold current and kink-free light output power-current (L-I) curve of the MQW violet InGaN LD with an emission wavelength near 405 nm, and to analyse the output of the LD for the purpose of digital modulation.

The performance of the MQW violet InGaN LD has been achieved through optimization of its active region, blocking layer (BL) and cavity length. The MQW violet InGaN LD with double quantum well (QW) has been used as a base structure. The effects of QW thickness, barrier thickness and type on the electrical and optical properties and built-in polarization have been investigated. The kink-free L-I curve with the lowest threshold (16.42 mA) and highest output power (64.2 mW) has been obtained with QW and barrier thicknesses of 2.5 and 5 nm, respectively. The built-in polarization has been proven to depend on the QW thickness and barrier thickness and type.

The influence of the quaternary AlInGaN BL on LD properties has been extensively investigated. The threshold current of the LD has reduced from 16.42 mA to 13.76 mA when considering the quaternary AlInGaN as a BL instead of the ternary AlGaN BL. The enhancement of carrier density distribution between double QW has been observed with quaternary AlInGaN BL.

The analysis of the output of the simulated MQW violet InGaN LD has been achieved and the LD parameters required for studying and analyzing the pulse response for digital modulation of the LD have been calculated through the output analysis, solving the LD rate equations, and some experimental works. The digital modulation items, which have been investigated and determined, are relaxation oscillation, frequency of relaxation oscillation, turn-on and turn-off times, bit rate and extinction ratio. The MQW violet InGaN LD with quaternary AlInGaN BL has exhibited better digital modulation characteristics than the LD with ternary AlGaN BL.

Overall, in this study, simulation results were found in line with several experimental studies in the literature.

CHAPTER 1

INTRODUCTION

1.0 Overview

Group III-nitrides based semiconductors have emerged as the leading materials for the production of blue-violet light emitting diodes (LEDs) and laser diodes (LDs). The historical evolution of GaN-based materials and devices technology in Japan, USA, and Europe in the early 1990’s is regarded as the most important developments in solid-state devices today.

Group III-nitride materials have been recognized as one of the most promising optoelectronic semiconductor materials because they possess excellent mechanical properties such as high melting point, high hardness, and high thermal conductivity. In addition, group III-nitride materials have large direct tunable band gaps which are appropriate for short-wavelength LEDs and LDs where the usefulness and goodness of GaN and its alloys have been well established for the fabrication from visible to ultraviolet (UV) LEDs and LDs.

Violet LD that is based on these materials, especially the LD with an emission wavelength near 405 nm has attracted great interest as a light source for high-density optical data storage, high-resolution color printing, chemical sensor, medical applications, and undersea optical communications.

Since the demonstration of the first InGaN/GaN LD by Nakamura et al. [1], significant progress has been made towards reducing the threshold current, increasing the output power, increasing the lifetime of the LDs and improving the device characteristics.

In spite of the significant progress achieved, many aspects regarding the technology of group III-nitrides-based LDs are in need to be improved. In addition, the underlying issues of physics must be clarified and that superior performances of shorter emission wavelengths are expected to be a form of challenges for the next-generation devices [2].

Group III-nitrides-based LDs are normally grown on the c-plane (0001) of the wurtzite crystal structure. Therefore, such LDs suffer from the presence of spontaneous and piezoelectric polarizations which induce a built-in electrostatic field resulting in significant reduction of electron-hole wavefunction overlap. Therefore, the radiative recombination rate and optical gain of the quantum well (QW) will be further reduced. Moreover, the lack of suitable native substrate leads to high threading dislocation density. This high threading dislocation density in group III-nitride materials leads to low radiative efficiency of the LDs. The indium segregation is another reason which causes the reduction of light emission [of the LDs] [3]. Furthermore, low quality and limited doping of the p-type are still problems in realizing high performance nitride based device [4]. Therefore, the present nitride-based LDs suffer from relatively high threshold current density between 2-4 kA/cm^2 [5].

On the other hand, GaN-based devices are known to operate very well without aging effects with dislocation density as high as 10^{10} cm^{-2}. In spite of this large number of dislocation in GaN-based LEDs and LDs, the efficiency of these devices is much higher than that of the conventional III-V compound semiconductors, such as AlGaAs and AlInGaP-based LEDs and LDs where many reports suggest that III-V nitride-based devices are less sensitive to dislocation than the conventional III-V semiconductors [6, 7]. Moreover, the lifetimes of blue-violet LDs have been improved to greater than 15 000 h under room temperature (RT) at continuous wave (CW) at 60 ^{o}C [8, 9].

The dynamics of the LD are studied through the use of well-known laser rate equations. Since these rate equations are non-linear, various linearization methods have been utilized [10].

LDs are important in information technology because of its high coherent light output, small size, ruggedness and high efficiency which can be modulated to carry code information at a high distance and speed via fiber optics. LDs can be modulated and tuned directly. The modulation is either digital or analog. Digital modulation is extremely important for most LD applications. Therefore, analytical applications such as undersea optical communication systems and blu-ray disc (BD) of the multi-quantum-well (MQW) violet InGaN LDs require a detailed knowledge about its pulse response and relaxation oscillation (RO) for the purpose of digital modulation. Pulse response and RO have been carefully studied for GaAs- and InP-based LDs for the optical communication systems. However, almost no information is available on the RO and pulse response analysis related to digital modulation for InGaN-based LDs.

1.1 Crystal structure of group III-nitrides

Group III-nitrides exist in three common crystal structures: the wurtzite, zincblende, and NaCl. Under ambient conditions, the thermodynamically stable structure is wurtzite for bulk aluminum nitride (AlN), gallium nitride (GaN), and indium nitride (InN) [11]. Wurtzite structure has a hexagonal unit cell and thus two lattice constants (c and a). Wurtzite structure consists of two interpenetrating hexagonal closely packed (HCP) sublattices; each one is with one type of atom, and offset along the c-axis by 5/8 of the cell height (c). Each group-III atom (Gallium (Ga)) is coordinated by four nitrogen (N) atoms and vice versa. Wurtzite GaN has two faces: Ga face (Ga-polarity) and N face (N-polarity). Figure 1.1 shows the crystalline structure: (a) hexagonal (wurtzite), (b) cubic, (c) and (d) represent Ga-polarity and N-polarity of wurtzite GaN, respectively [12]. It can be seen that the directions of spontaneous polarization are also designated as arrows as in c and d.

Wurtzite GaN, InN and AlN crystals have bonds along the c-axis which are longer than the other bonds. Therefore, this non-ideality which is given by the differences in bond lengths and the ionicity of the Ga-N bond leads to the existence of a non-zero electrical dipole moment which is parallel to the c-axis, and consequently to a spontaneous polarization [11]. The spontaneous polarization in group III-nitrides is very large in terms of MV/cm and that the increase from GaN to InN and AlN is due to the increase of the non-ideality of the crystal structures.

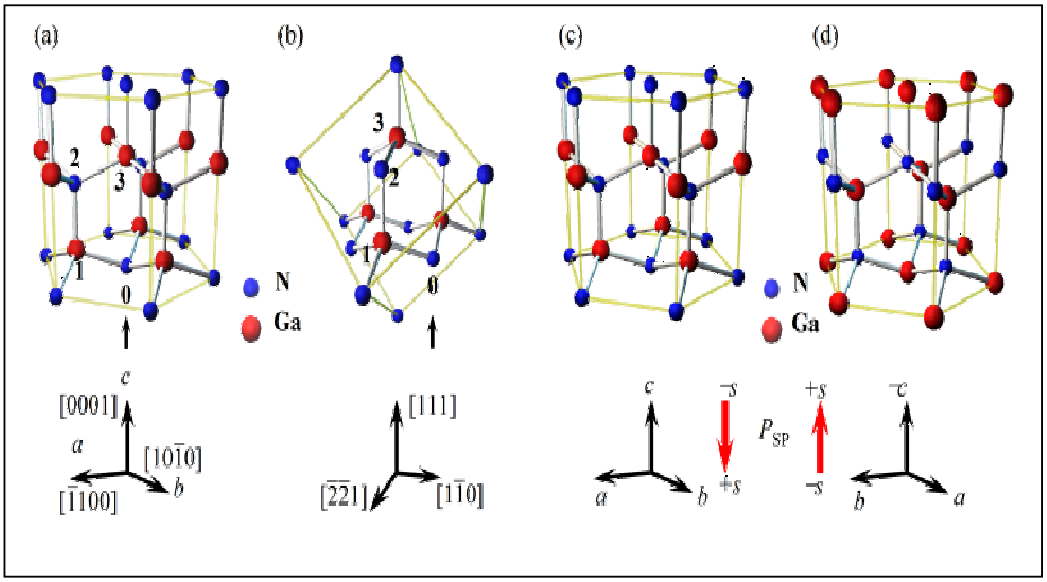

Figure 1.1. The crystalline structure of (a) hexagonal, (b) cubic, (c) Ga-polarity and (d) N-polarity of GaN. Directions of spontaneous polarization are also designated as arrows in (c, d) [12].

1.2 Unique properties of group III-nitrides

Group III-nitrides, AlN, GaN, InN, and their alloys are considered materials of great interest for the applications in optoelectronic devices. This is due to their wide and direct band gap ranging from 0.77 eV for InN to 3.4 eV for GaN and to 6.2 eV for AlN. Therefore, these materials together with their ternary alloys InGaN and AlGaN can, in principle, cover almost all the visible and near-ultraviolet regions of the spectrum as schematically depicted in Figure 1.2 [13]. Figure 1.2 plots the band gap energies and wavelengths of group III-nitrides and some semiconductor compounds and elements as functions of their lattice constants. Moreover, group III-nitride materials are also characterized by unique properties such as: high thermal and chemical stability, low compressibility, high breakdown field (1.5×10^6 V/cm), high thermal conductivity (1.3 W/cm ^{o}C) [14], and high melting temperature (for GaN 2540 K) [15]. Therefore, these properties make group III-nitrides one of the most promising candidates as potential materials for the applications to LEDs and LDs from near-ultraviolet to the visible region of the spectrum.

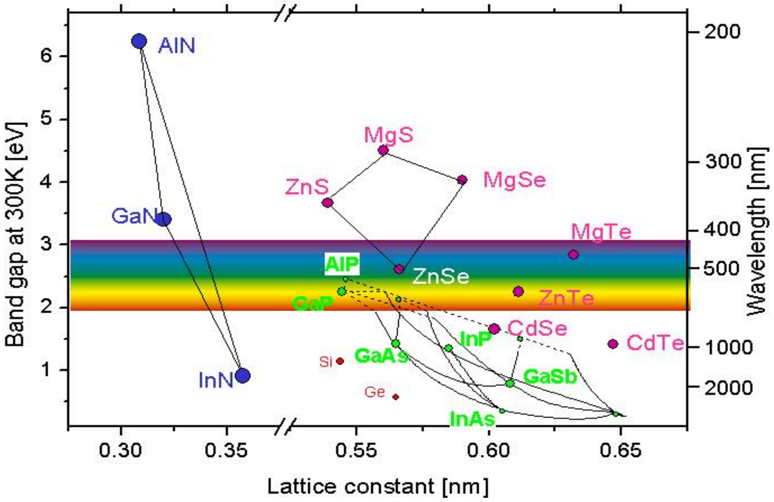

Figure 1.2. Diagram of the band gap energies and wavelengths of group III-nitrides and some semiconductor compounds and elements as functions of their lattice constants [13].

1.3 Problems of group III-nitrides

Although group III-nitride materials have potential properties as mentioned above, these properties also make the growth of high-quality single crystals, the epitaxy of perfect layers and the device processing difficult and complicated [11]. The problems are discussed in the subsequent sub-sections.

1.3.1 Mismatch

Mismatch between group III-nitrides and the substrates and among group III-nitrides themselves is considered a major problem when working with these materials. Heteroepitaxial growth of GaN is usually performed on sapphire or SiC substrates with lattice mismatch 13% and 3.5%, respectively [16]. Two important crystal properties that should be ideally closely matched between GaN and the substrate; these are the lattice parameters and the coefficient of the thermal expansions. Any mismatch between these properties can result in defects in the film. This means that the misfit and threading dislocations are due to the lattice mismatch; and that cracking or bowing is due to the thermal mismatch.

The lack of suitable native substrates leads to a poor quality epitaxial GaN film with dislocation density as high as 10^{10} cm^{-2} when growing on a sapphire or SiC substrates. The low thermal conductivity and insulating properties make sapphire less perfect as a substrate for the GaN epilayers; while the high cost and some of the mechanical defects of the SiC hinder its acceptability in LEDs [and LDs] markets [17]. An ideal substrate for GaN epitaxy would be a high quality GaN wafer itself. However, this approach is limited due to the difficulties in producing sufficient high quality GaN substrate [18].

A variety of techniques has been employed to reduce this high dislocation density. One method was used to engineer the substrate surface to control the threading dislocation density, and thus inhibiting the formation threading dislocation and reducing the mismatch. This has been made by using the epitaxial lateral overgrowth (ELO) technique as it has been further proven to be used effectively to obtain low dislocation density as low as 10^6 cm^{-2} with estimated lifetime for LDs of 15 000 h [8, 9]. However, this technique is difficult and complex. Another approach which has attracted a lot of attention and it is considered easy; the growth of GaN is made on sapphire, SiC or silicon (Si) substrates by using AlN or GaN as nucleation layers [19]. By using these nucleation layers, it has become possible to obtain high-quality GaN films, a low residual carrier concentration, a high mobility and strong photoluminescence (PL) intensity even though there is a large lattice mismatch between GaN and these substrates [8].

On the other hand, the mismatch among group III-nitrides themselves leads to piezoelectric polarization when they are grown on a c-plan of the wurtzite structure. This will be elaborated below (see sub-section 1.3.2).

1.3.2 Polarization

It is well known that a strong built-in polarization inside the epitaxial structures of group III-nitrides influences their device properties. This built-in polarization is due to piezoelectric and spontaneous polarizations. Piezoelectric polarization is formed when the materials with different lattice constants come together, such as $In_xGa_{1-x}N$ well with GaN barrier layer. The discontinuity in polarization from one material to another creates bound charges at the interfaces which, in turn, lead to quantum confined stark effect (QCSE) [20]. QCSE creates band bending in the quantum well (QW) as indicated in Figure 1.3, and this leads to make the electrons in the conduction band move to a side; while the holes in the valence band move to the other side of QW. On the other hand, spontaneous polarization, as mentioned previously, existed due to the electrical field in the intrinsic material. Consequently, the total polarization is equal to the sum of spontaneous and piezoelectric polarizations. Polarization leads to increase in the threshold current, and reduce the output power and efficiency of the InGaN-based LDs. In fact, polarization exists in the c-plane of group III-nitrides of wurtzite structures; while such polarization does not exist in the m-plane of wurtzite structure, as can be seen in Figure 1.3 [21]. Therefore, c-plane is called polar plane; while m-plane is called non-polar plane. Recently, the idea of achieving a structure that is free from built-in electrostatic field in non-polar direction has been proposed [22-25]. However, the appropriate growth orientation for non-polar is still under investigation and development and the growth condition may be much more complicated as compared to the conventional growth process [26].

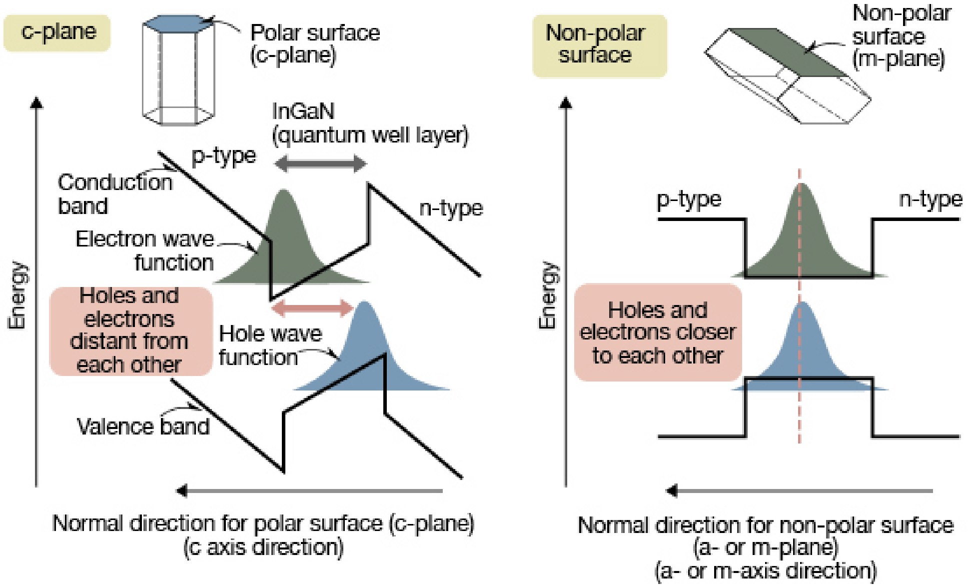

Figure 1.3. Polar (c-plane) and non-polar (m-plane) of group III-nitrides of wurtzite structure [21].

1.3.3 Indium composition

Ternary $In_xGa_{1-x}N$ alloy is widely used as an active layer in InGaN-based LEDs and LDs. The main problem with InGaN is the growth temperature where a lot of experimental works have proven that growing high quality InGaN is very difficult, especially for high indium (In) composition in $In_xGa_{1-x}N$ alloy [27]. In order to grow QW with high In content, the growth temperature for the InGaN QW needs to be lowered, taking into account the low sticking coefficient of In which results in lower crystalline quality in the QW and barrier [28]. Such growth conditions often result in compromised material quality in the MQW and barriers which are also associated with a poor optical quality of the active region and formation of the localized states by phase separation [29]. Besides temperature, indium incorporation is also strongly dependent upon the growth rate, pressure, carrier gas and V/III ratio [30].

Moreover, as In composition increases, the lattice-mismatch induces increased strain of InGaN epitaxy on GaN which leads to cause a variety of defects to the materials. Therefore, one can see that the low In-content in ternary $In_xGa_{1-x}N$ alloy is widely used as an active layer to fabricate high-brightness blue-violet LEDs and LDs.

Furthermore, the weakness of the In-N bond requires the growth temperature of InGaN to be reduced [31].

1.3.4 P-type doping

Controlled p-type doping is crucial for the development of group III-nitrides as it is used in visible and ultraviolet LED and LD devices. The first successful p-type of GaN was achieved by Amano et al.; they used magnesium (Mg) as a dopant with low-energy electron-beam irradiation (LEEBI) treatment [32]. A few years later, Nakamura et al. obtained p-type conductivity by removing hydrogen which passivates the Mg acceptor through thermal annealing [33]. However, this method allows only a fraction of the total Mg dopant to be activated [34, 35].

Despite that Amano et al. and Nakamura et al. have showed that Mg can be used as a dopant, but it is far from being ideal. Mg is an acceptor in GaN residing between 180 and 250 meV from the valence band edge making ionization difficult at room temperature [36]. This problem is greater at short wavelength and higher aluminum composition [as in AlGaN blocking layer of LD where a higher Al composition is always needed] due to further deepening of this center [36, 37].

For p-type GaN, there are still some challenges, such as low hole concentration and mobility which result in a high device resistivity [38]. Moreover, some theoretical and experimental studies indicated that compensation by natural defects plays a significant role in the p-type doping process [39]. Therefore, p-type doping in GaN [and its alloys] is much more complicated than that of n-type doping [36].

1.4 Advantages of violet laser diode near 405 nm

Violet InGaN LDs with an emission wavelength near 405 nm have many advantages such as high efficiency, relatively high power and low threshold current.

In addition, violet InGaN LDs with an emission wavelength near 405 nm have potential applications in blu-ray disc (BD) to read and write data. The blu-ray disc is expected to be used in the next-generation recording technology beyond digital versatile disc (DVD). It dramatically increases recording density by using a violet 405-nm laser compared to the conventional 650-nm red laser used in today's DVD technology. The shorter wavelength allows a smaller spot size and track pitch to be recorded on the disc, increasing storage density from 4.7 to 25 GB on one side of the disc [6].

In reality, blu-ray disc overcomes DVD-reading issues by placing the data on top of a 1.1-mm-thick polycarbonate layer [40]. Since the data is on top of the BD, this prevents birefringence and therefore prevents readability problems. Moreover, the recording layer is placed closer to the objective lens of the reading mechanism, the problem of disc tilt is virtually eliminated; because the data is closer to the surface, a hard coating is placed on the outside of the disc to protect it from scratches and fingerprints [40]. Figure 1.4 shows CD and DVD versus BD.

Moreover, violet LDs can also improve the performance of laser display, color printer, medical applications and undersea optical communication systems.

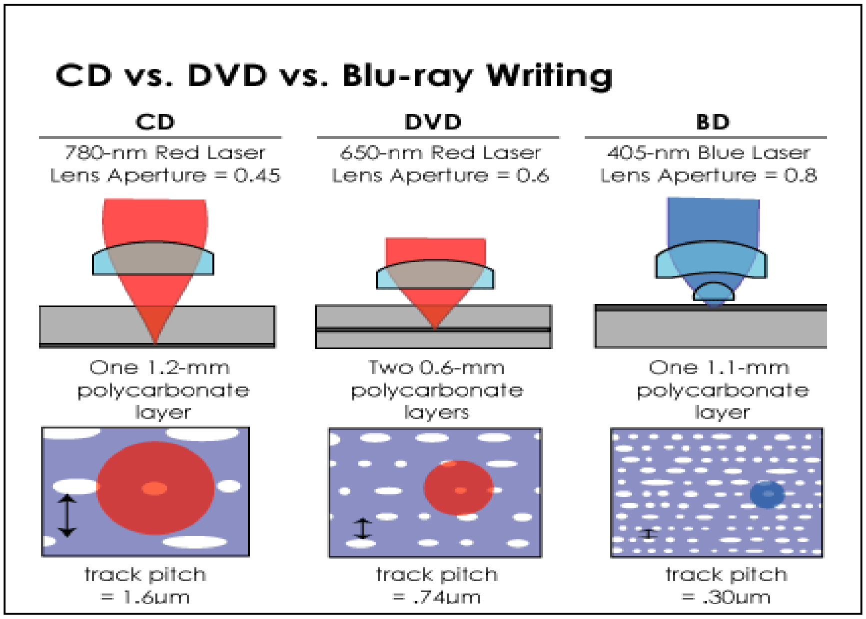

Figure 1.4. CD and DVD versus BD [40].

1.5 Double quantum well blue-violet InGaN laser diodes

Several experimental and simulation studies indicated that double quantum well (DQW) blue-violet InGaN LDs have many advantages, such as higher output power and efficiency with lower threshold current, depending on the specific wavelength of the LDs.

Nakamura et al. experimentally studied the performance of several LDs with an emission wavelength of 390-420 nm as a function of the number of InGaN well layers. They found that the lowest threshold current density is obtained when the number of InGaN well layers is two [41]. However, in another study, they observed that LDs with an emission wavelength longer than 435 nm and when the number of InGaN well layers varies from one to three, the threshold current density is the lowest at one, and increased with the number of InGaN well layers [42]. In another study, when the number of the InGaN well varies between 1 and 4, with an emission wavelength of the LDs around 408 nm, Nakamura et al. found that the lowest threshold current density is obtained with DQW of the LD [43]. This phenomenon is attributed to the dissociation of the high indium content of InGaN QW at high growth temperature [44].

On the other hand, several simulation studies [45-50] were in line with Nakamura’s experimental studies as will be discussed below.

J. Y. Chang and Y. K. Kuo studied laser performance with an emission wavelength of 462 nm. They found that the threshold current density increases with the number of well layers. They also found that the hole distribution is non-uniform between DQW and this non-uniform hole distribution plays an important role in laser performance as a function of the number of well layers and that the performance decreases when the number of well layers increases [45].

Y. K. Kuo et al. studied the characteristics of the blue-violet MQW InGaN LDs with an emission wavelength of 400-480 nm when the band-offset ratio of the $In_xGa_{1-x}N/In_yGa_{1-y}N$ heterojunction is 3/7 and 7/3. They found when the band-offset ratio is 7/3, the lowest threshold current of the blue-violet InGaN LD is obtained when the number of well layers is two if the emission wavelength is shorter than 450 nm, and one if the emission wavelength is longer than 450 nm [46].

Y. K. Kuo and Y. A. Chang investigated laser performance of several MQW InGaN LDs with an emission wavelength of 392-461 nm. Their simulation results indicated that the lowest threshold current density is obtained when the number of QW is two if the emission wavelength is shorter than 427 nm, and one if the emission wavelength is longer than 427 nm [47].

Optical properties of the MQW InGaN violet and ultraviolet LDs were numerically studied by S. H. Yen et al.; especially, the performance of the LDs of various active region structures operating in a spectral range from 385 to 410 nm. Their simulation results indicated that the DQW laser structure with a peak emission wavelength of 385-410 nm has the lowest threshold current [48].

S. M. Thahab et al. studied the effect of QW number on the output power, threshold current and slope efficiency of MQW InGaN LDs with an emission wavelength around 416 nm. They observed a maximum output power, a higher slope efficiency, and a lower threshold current when the number of QW is two [49, 50].

The above mentioned simulation studies indicated that the dissociation of the InGaN QW during crystal growth is not the only cause for the deterioration of laser performance when number of QW is over than two because the respective researchers did not take into account the dissociation of the InGaN QW during crystal growth in their software simulation programs. They suggested that the non-uniform hole distribution plays an important role in the laser performance due to the large mass and low mobility of the hole, high band offset in the valence band, and using the high band gap blocking layer which result in accumulating the holes in the QW near p-type of the LD structure.

On the other hand, it has been discussed that the blue InGaN LDs have peculiar temperature characteristics due to the unique carrier transport properties of DQW InGaN with high In composition which is deduced from the simulation of carrier density and optical gain [51]. The DQW LD structures with an emission wavelength 445 nm having an n-type doped barrier show negative or very high temperature characteristics depending on the In barrier composition [51]. On the contrary, the DQW structures having an undoped barrier and a single QW structure show normal dependence of LD temperature characteristics [51]. In another study, H. Y. Ryu et al. reported high stable temperature characteristics of the threshold current and output power in InGaN blue LDs emitting around 450 nm [52]. The threshold current is changed by <3 mA in operation temperature range from 20 to 80 °C, and even negative temperature characteristics was observed in a certain temperature range [52].

1.6 The quaternary $Al_xIn_yGa_{1-x-y}N$ alloy in the InGaN laser diodes

The quaternary $Al_xIn_yGa_{1-x-y}N$ alloy is potential for the fabrication of lattice matched III-nitride by independently controlling the band gap energy and the lattice constant and it has better lattice match to GaN resulting in a decrease of dislocations [53, 54]. Moreover, the use of $Al_xIn_yGa_{1-x-y}N$ quaternary materials is proved to be a promising approach in realizing deep UV devices [55].

The growth temperature of quaternary AlInGaN by metal organic chemical vapor deposition (MOCVD) ranges from 750 to 900 ^{o}C [53, 56, 57]; and this is close to the growth temperature of the InGaN active region. As a result, this makes the indium prevention by evaporation from the InGaN active region better when using it as a blocking layer (BL) than using the conventional ternary AlGaN BL.

Theoretically, J. R. Chen et al. showed that the built-in polarization can be reduced by using quaternary AlInGaN as a BL instead of ternary AlGaN BL [58]. The optical properties of InGaN MQW LDs with different polarization-matched AlInGaN barrier layers have been investigated numerically by S. Park et al. [59]. These researchers showed that the use of quaternary polarization-matched AlInGaN barrier layers enhances the electron-hole wavefunction overlap due to the compensation of polarization charges between InGaN QW and AlInGaN barrier layer. The optimal polarization-matched InGaN/AlInGaN LD showed lower threshold current and higher slope efficiency compared to the conventional $In_xGa_{1-x}N/In_yGa_{1-y}N$ LDs. C. Skierbiszewski et al. used the quaternary AlInGaN in the superlattice cladding layer of the LD as AlInGaN/InGaN pairs instead of conventional AlGaN/GaN pairs; they relatively obtained high output power (60 mW) at room temperature [60].

Therefore, the quaternary AlInGaN alloy is indeed the most promising material to be used as a BL because it better matches with the InGaN and GaN barriers in the active region and it independently controls the band gap energy and the lattice constant parameters.

1.7 Digital modulation of violet InGaN laser diodes

The InGaN LDs near 405 nm are expected to play an important role in undersea optical communication systems, especially after increasing their lifetimes where long lifetime is always needed for laser used in optical communication systems. Moreover, the digital modulation of the pulse response of violet InGaN LDs is also required in other applications. Therefore, the analysis of digital modulation and pulse response of violet InGaN LD are required to examine the ability of this laser to build a clean square wave of pulse response. The other items of the digital modulation of violet InGaN LD such as relaxation oscillation (RO), turn-on and turn-off times, and bit rate have not been sufficiently clarified yet.

However, there is very little information about the digital modulation of violet InGaN LDs. The violet InGaN LDs have been modulated with pulse current in order to measure the carrier lifetime experimentally by S. Nakamura et al. and M. Kuramoto et al. [61-63]. M. Kuramoto et al. studied the relationship between the slope gain and frequency of the relaxation oscillation of the violet InGaN LDs with emission wavelengths at 411, 404 and 397 nm. They observed the ROs in the pulse response for these three LDs and concluded that the LD which has higher RO, also has a higher carrier lifetime [63]. S. Nakamura et al. modulated the MQW violet InGaN LD with an emission wavelength near 405 nm, and they measured the frequency of the RO which was 3 GHz [64].

1.8 Research objectives

The objectives of this simulation and theoretical research are:

1. To design low threshold kink-free light output power-current (L-I) curve of MQW violet InGaN LD with an emission wavelength around 405 nm by using **ISE TCAD** (**I**ntegrated **S**ystem **E**ngineering **T**echnology **C**omputer **A**ided **D**esign) simulator
2. To optimize the active region of the MQW violet InGaN LD with an emphasis on reducing the polarization effects
3. To use the quaternary AlInGaN as a BL instead of the conventional ternary AlGaN BL
4. To study and analyze the output of the MQW violet InGaN LD with ternary AlGaN and quaternary AlInGaN BLs
5. To study and analyze the pulse response of the digital modulation of the MQW violet InGaN LDs using MATLAB program based on linearization of the rate equations by applying Jacobian matrix and state-space model

1.9 Research originality

The originality of this research can be summed up as listed below:

1. Designing edge emitting MQW violet InGaN LDs with low threshold current and relatively high power without using ridge geometry and superlattice cladding layers
2. Reducing and exploring new influences of built-in polarization on the MQW violet InGaN LDs
3. Exploring the quaternary AlInGaN BL in the LD to enhance optical intensity and carrier density distribution inside the active region

4. Proposing a novel model for simulation of digital modulation by coupling ISE TCAD simulator with MATLAB program
5. Using the proposed model for simulation and analysis of the pulse response for digital modulation of the MQW violet InGaN LDs which have not been studied before

1.10 Thesis outline

This study comprises of six chapters; they are outlined below:

Chapter 1 sets up the study by commencing with an overview on the topic. Then it moves to identify the advantages and problems of group III-nitride materials. The literature review is also presented in this chapter. The research objectives, originality of this research, and the thesis outline are presented in this chapter

Chapter 2 presents the relevant theories and concepts of the LDs that are utilized in this study

Chapter 3 explains the methodology that is employed in this study. Two simulation programs have been utilized and described in this chapter: ISE TCAD simulator and MATLAB program. Coupling ISE TCAD simulator with MATLAB program is also presented in this chapter

Chapter 4 presents the results and discussion of the performance of the MQW violet InGaN LDs

Chapter 5 presents the results and discussion of the output analysis and digital modulation of MQW violet InGaN LDs

Chapter 6 presents the conclusions of this study. The recommendations for future work are also proposed in this chapter

CHAPTER 2

THEORETICAL FRAMEWORK

2.0 Introduction

Theories and concepts of LD and group III-nitride materials that are related to this work will be explained in this chapter. The concepts of quantum confinement, quantum well, multi-quantum-well, and superlattice will be presented. The InGaN-based LD structure will be explained. Piezoelectric polarization and strain effects on the active region of the InGaN-based LD will be presented; and nitride materials rules will also be presented. The method of extracting the parameters of laser cavity-length dependent will be described and the temperature characteristics will also be included in the discussion to reveal its meaning and usefulness in the LD. The LD rate equations will be described and their meaning and usages will be explained. The pulse response for digital modulation purposes and its related concepts will be described.

2.1 Quantum well confinement

A quantum-confined structure is one in which the motion of the electrons or holes are confined in one or more directions by potential barriers [65]. The classification of quantum confinement is given in Table 2.1.

Table 2.1. The quantum confinement classification.

Structure	Confined directions	Freedom directions
Quantum well	1	2
Quantum wire	2	1
Quantum dot	3	0

Quantum size effects become important when the thickness of the layer becomes comparable with de Broglie wavelength of the electrons or the holes in the target material where quantum-mechanical effects are expected to occur. In this case, the distribution of low energy, wave-like states available for the electrons and holes confined to the active layer changes from quasi-continuous to discrete [66]. If we consider the free thermal motion of a particle of mass (*m*) in the z-direction, de Broglie wavelength at a temperature (*T*) is given by [65]:

$$\lambda_{de.} = \frac{h}{\sqrt{mkT}} \tag{2.1}$$

where *k* is Boltzmann constant. In general, in order to observe the quantum-confinement effects at room temperature for semiconductor materials, the thickness of the confined materials should be in a few nanometers. This thickness can easily be obtained by the molecular beam epitaxy (MBE) or MOCVD techniques.

The quantum well is a single layer of one narrow band gap ($E_{g(QW)}$) semiconductor which is sandwiched between two layers of a wider band gap material ($E_{g(barrier)}$), such as $In_xGa_{1-x}N$ as a well and GaN as a barrier, or from one material but with different mole fractions in the well and barrier, such as $In_{0.12}Ga_{0.88}N$ as a well and $In_{0.01}Ga_{0.99}N$ as a barrier where the condition $E_{g(Barrier)} > E_{g(QW)}$ must be inquired. Figure 2.1 represents the principle of QW confinement structure. The confinement direction in QW is usually taken in the z-direction.

The quantization of the motion in the z-direction (QW confinement) has three main results [65]. Firstly, the quantization energy shifts the effective band edge to a higher energy. Secondly, the confinement keeps the electrons and holes closer together and hence it increases the probability of radiative recombination rate. Finally, the density of states becomes independent of energy. Many useful properties of the QW follow these three properties. Therefore, the applications of the QW structures of LDs have received considerable attention because of its physical interest as well as its superior laser characteristics.

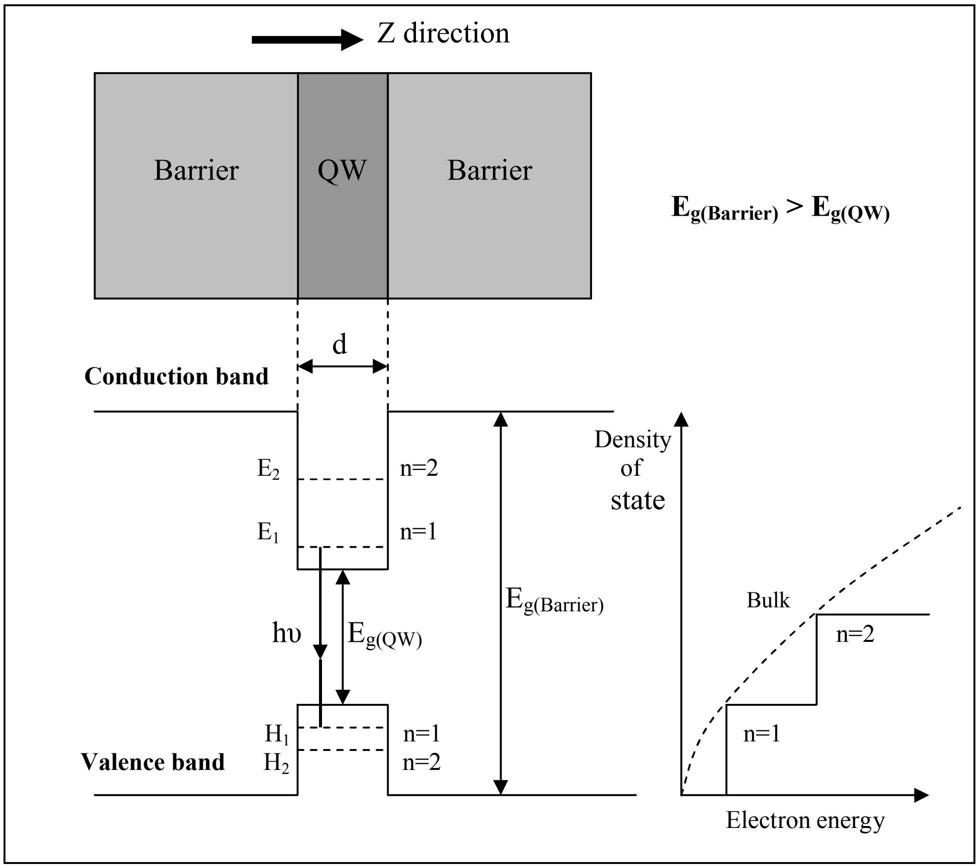

Figure 2.1. Principle of quantum well confinement structure.

From Schrödinger equation, the energy of the confined states for electrons and holes is given as:

$$E_{n,p} = \frac{\hbar^2 \pi^2 n^2}{2m^* d^2} \tag{2.2}$$

where n is the quantum number, $\hbar = \frac{h}{2\pi}$, h is Planck constant, d is the QW thickness, and m^* is the effective mass of the particle (electron or hole) in the QW.

Since the emission wavelength of a semiconductor corresponds to its band gap energy, custom-designed energies can be obtained where the energy emission from QW is [67]:

$$h\nu = E_{g(QW)} + E_1 + H_1 \tag{2.3}$$

where E_1 and H_1 are the state energies at n=1 of the electron and hole, respectively.

2.2 Multi-quantum-well and superlattice

The MQW structure has the same single QW structure, but it consists of more than one QW alternative layers with relatively thick barriers which prevent the tunneling between the wells and barriers and thus the carriers become very dense inside the quantum well. The MQW is used as an active region in the LD where the laser takes place. Hence, a higher power of the LD can be produced by using MQW as an active region than the single QW active region. MQW structure is shown in Figure 2.2 (a).

A superlattice (SL) is very thin alternative layers of two materials. The purpose of the SL is to take advantage of the tunneling properties associated with crystal lattice systems and controlling the movement of the carriers [65]; while still maintains control over the design of band gap energy. In fact, the SL is similar to MQW, but the barrier thickness is smaller, when the barrier thickness is reduced, the wave functions of adjacent wells begin to overlap and the discrete levels broaden to minibands as the wave functions in neighboring wells couple together through the thin barrier that separates them [65], as shown in Figure 2.2 (b). The SL can be used as many pairs in the cladding layers to eliminate the mismatch problem and to increase the optical confinement inside the active region of LD. The common SL feature in InGaN-based LDs is AlGaN/GaN pairs.

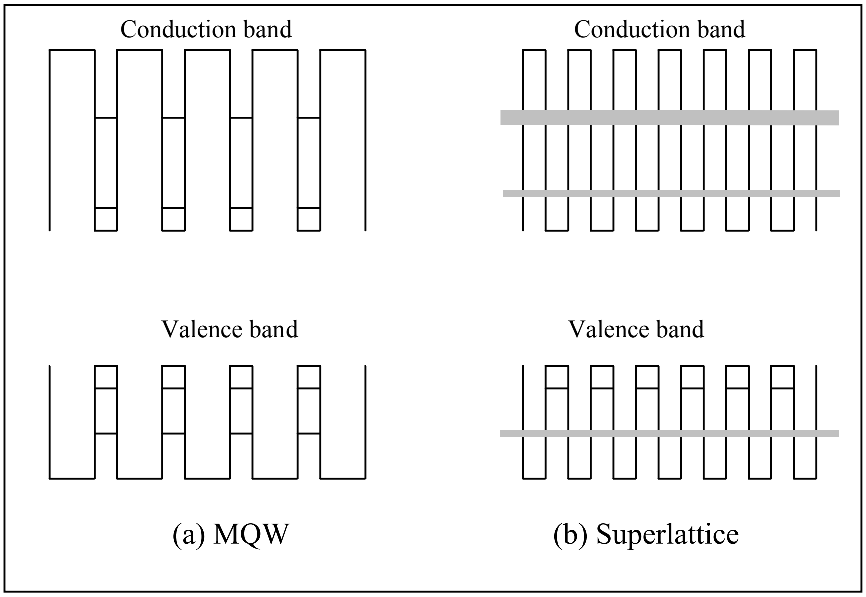

Figure 2.2. The MQW and superlattice structures.

2.3 InGaN-based laser diode structure

The state of art in InGaN-based LDs is realized as separate confinement heterostructure multi-quantum-well (SCH-MQW) lasers. The SCH is a modification of the double-heterostructure (DH) which provides additional carrier confinement. This confinement plays an important role in the III-nitrides based optoelectronic devices where a better confinement of the injected electrons is considered as a key issue to be resolved due to the low efficiency of p-type doping in these materials [68].

A vertical structure of such an LD can be seen in Figure 2.3. The active region of such a device consists of several $In_xGa_{1-x}N/GaN$ or $In_xGa_{1-x}N/In_yGa_{1-y}N$ MQW placed in the junction region of a p-n heterostructure which is sandwiched on both sides by the layers having higher band gap energies, i.e. the top and bottom waveguides and cladding layers.

The QWs are designed to trap electrons in a two-dimension environment and to have a particular band gap energy related to the wavelength of the light emitted by the LD. The QW allows the electrons to gather more densely in the well than they would elsewhere. This can be achieved by the band discontinuities in the conduction and valence bands which confine the electrons and holes within the active region. This results in more concentrated carriers as compared with the usual homogenous structure where carriers can be diffused over distances of the orders of microns.

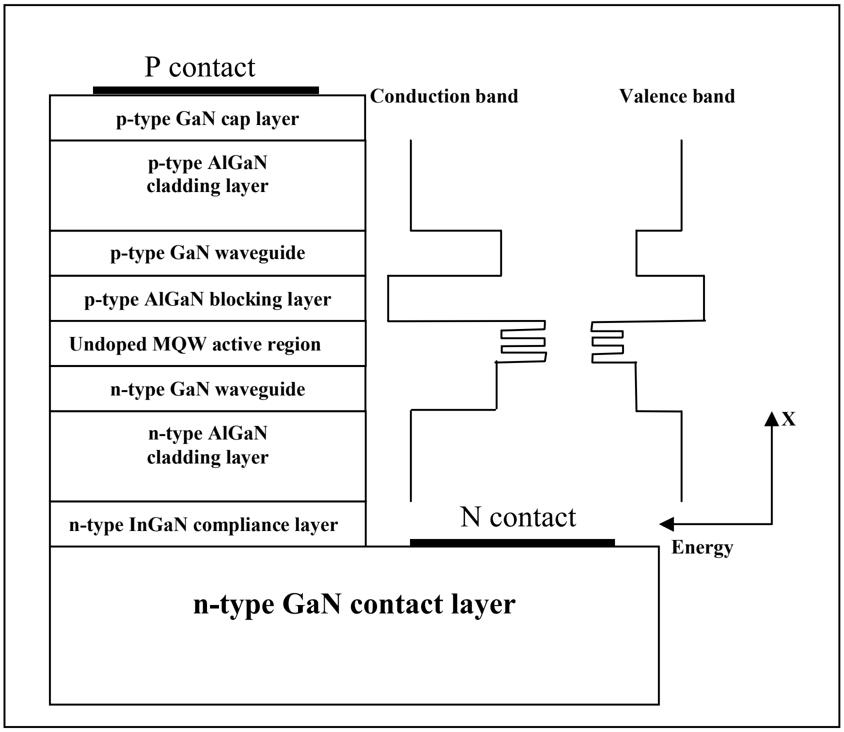

Figure 2.3. Diagram of SCH-MQW laser diode structure [1].

By using a convenient semiconductor feature, increasing the band gap energy of the semiconductor by changing its composition also normally decreases its refractive index. This leads to optical confinement of the photons closely around the active region. The larger refractive index of the inner layer in the heterostructure guides the optical wave between the outer layers (cladding layers). However, to realize the confinement in an optimal way, the optical waveguide should have a relatively large thickness. For this reason, the waveguide is normally thicker than the active region, and the cladding layers of the LD, which are surrounding the waveguide, are always thicker than the waveguide. Consequently, in accordance with Snell's law, the light will be confined in the active region. This is similar to the optical properties of a fiber optic cable. This can be seen in Figure 2.4 which represents rays and intensity confinement in the LD. Where n is the refractive index, n_1 and n_2 are the refractive indices of the waveguide and cladding layers, respectively.

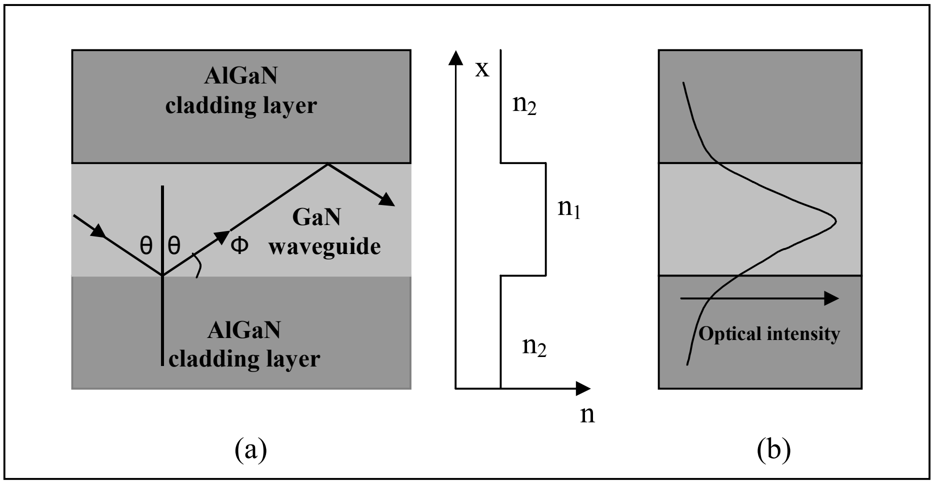

Figure 2.4. Rays and intensity confinement in the laser diode [11].

However, only a small part of the light field that oscillates along the QWs is confined in the active region because the active region is very thin in comparison with other parts of the laser structure. The thickness of the active region depends on the thicknesses and number of QWs and barriers. In the InGaN-based LDs, the normal thickness of the active region with DQW is around 20 nm. Therefore, the